blood

2010 116: 2847-2856
Prepublished online Jun 29, 2010;
doi:10.1182/blood-2010-03-274258

Nanoparticle-induced vascular blockade in human prostate cancer

Lilach Agemy, Kazuki N. Sugahara, Venkata Ramana Kotamraju, Kunal Gujraty, Olivier M. Girard, Yuko Kono, Robert F. Mattrey, Ji-Ho Park, Michael J. Sailor, Ana I. Jimenez, Carlos Cativiela, David Zanuy, Francisco J. Sayago, Carlos Aleman, Ruth Nussinov and Erkki Ruoslahti

Blood (print ISSN 0006-4971, online ISSN 1528-0020), is published semimonthly by the American Society of Hematology, 1900 M St, NW, Suite 200, Washington DC 20036.

Nanoparticle-induced vascular blockade in human prostate cancer

Lilach Agemy,[1] Kazuki N. Sugahara,[1] Venkata Ramana Kotamraju,[1] Kunal Gujraty,[1] Olivier M. Girard,[2] Yuko Kono,[2] Robert F. Mattrey,[2] Ji-Ho Park,[3] Michael J. Sailor,[3] Ana I. Jimenez,[4] Carlos Cativiela,[4] David Zanuy,[5] Francisco J. Sayago,[4] Carlos Aleman,[5] Ruth Nussinov,[6,7] and Erkki Ruoslahti[1,8]

[1]Vascular Mapping Laboratory, Center for Nanomedicine, Sanford-Burnham Medical Research Institute at the University of California at Santa Barbara (UCSB), Santa Barbara, CA; [2]Department of Radiology, University of California, San Diego, CA; [3]Materials Science and Engineering Program and Department of Chemistry and Biochemistry, University of California, San Diego, La Jolla, CA; [4]Organic Chemistry Department, Instituto de Ciencia de Materiales de Aragon (ICMA), University of Zaragoza–Instituto de Carboquimica (CSIC), Zaragoza, Spain; [5]Department of Chemical Engineering, Escola Técnica Superior d'Enginyers Industrials de Barcelona (ETSEIB), Polytechnic University of Catalonia, Barcelona, Spain; [6]Basic Science Program, Center for Cancer Research Nanobiology Program, SAIC-Frederick, National Cancer Institute, Frederick, MD; [7]Department of Human Genetics, Sackler Medical School, Tel Aviv University, Tel Aviv, Israel; and [8]Cancer Research Center, Sanford-Burnham Medical Research Institute, La Jolla, CA

The tumor-homing pentapeptide CREKA (Cys-Arg-Glu-Lys-Ala) specifically homes to tumors by binding to fibrin and fibrin-associated clotted plasma proteins in tumor vessels. Previous results show that CREKA-coated superparamagnetic iron oxide particles can cause additional clotting in tumor vessels, which creates more binding sites for the peptide. We have used this self-amplifying homing system to develop theranostic nanoparticles that simultaneously serve as an imaging agent and inhibit tumor growth by obstructing tumor circulation through blood clotting. The CREKA nanoparticles were combined with nanoparticles coated with another tumor-homing peptide, CRKDKC, and nanoparticles with an elongated shape (nanoworms) were used for improved binding efficacy. The efficacy of the CREKA peptide was then increased by replacing some residues with nonproteinogenic counterparts, which increased the stability of the peptide in the circulation. Treatment of mice bearing orthotopic human prostate cancer tumors with the targeted nanoworms caused extensive clotting in tumor vessels, whereas no clotting was observed in the vessels of normal tissues. Optical and magnetic resonance imaging confirmed tumor-specific targeting of the nanoworms, and ultrasound imaging showed reduced blood flow in tumor vessels. Treatment of mice with prostate cancer with multiple doses of the nanoworms induced tumor necrosis and a highly significant reduction in tumor growth. (*Blood*. 2010; 116(15):2847-2856)

Introduction

The prevalence of prostate cancer and the large number of deaths due to this disease underscore the need for a paradigm shift in strategies to better treat this cancer.[1] Since the 1970s, progress in fundamental cancer biology has led to enormous advances in our understanding of the processes that underlie malignant transformation and metastatic dissemination. Nonetheless, eradication of cancer remains an elusive clinical goal, largely because of the heterogeneous nature of individual cancers and our inability to target therapies to neoplastic cells without damaging normal tissues. Prostate tumors are anatomically, histologically, and genetically heterogeneous,[2-4] which causes variable responses to various therapies. These obstacles are further magnified by our limited ability to image cancerous regions and track the progression of treatments.[5,6]

One approach to overcome the heterogeneity of tumors is to focus on tumor vasculature. Tumor vasculature has proven to be particularly well suited as a site for homing-based (synaphic) targeting. It expresses a multitude of molecules that are not expressed in the vessels of normal tissues, and the vascular wall is readily accessible for blood-borne substances.[7] Most vascular strategies use antiangiogenic therapy to prevent formation of new blood vessels in a growing solid tumor; these approaches have been found to be useful, particularly in treating advanced-stage cancers.[8-12] An alternative strategy is based on occluding the vasculature of a tumor and thereby inducing tumor necrosis. Targeting of truncated tissue factor to tumors has been used for this purpose with some success.[13-17] Nanomedicine is an emerging field that uses nanoparticles to facilitate the diagnosis and treatment of diseases. Nanoparticles can be engineered to perform multiple functions, which provides a potential advantage over simple drugs. In the present study, we designed nanomedicine-based approaches to more effectively and safely block the tumor circulation.

Our laboratory screens phage-displayed peptide libraries in vivo and ex vivo to discover specific targets in tumor vessels.[18] Some of the tumor-homing peptides we have identified in this manner recognize products of blood clotting on the walls of tumor vessels and in tumor stroma that are not present in normal vessels and tissues. The reasons for this difference are thought to be a procoagulant tumor environment and seepage of plasma proteins, including fibrinogen, from the leaky tumor vessels into the tissue.[19,20] We have identified 3 tumor-homing peptides that recognize these clotting products in the vessels of a variety of tumor types, including human cancers.[21,22] Tumors grown in mutant mice null for fibrinogen or in mice lacking plasma fibronectin, which becomes covalently bound to fibrin during blood clotting, are not recognized by these peptides, which indicates that the peptides target fibrin-fibronectin complexes.

Submitted March 10, 2010; accepted June 3, 2010. Prepublished online as *Blood* First Edition paper, June 29, 2010; DOI 10.1182/blood-2010-03-274258.

The online version of this article contains a data supplement.

The publication costs of this article were defrayed in part by page charge payment. Therefore, and solely to indicate this fact, this article is hereby marked "advertisement" in accordance with 18 USC section 1734.

We have recently used one of the peptides that recognize fibrin-fibronectin complexes, a pentapeptide with the sequence Cys-Arg-Glu-Lys-Ala (CREKA), to design a self-amplifying nanoparticle-delivery system.[22] Iron oxide nanoparticles coated with this peptide accumulate in tumor vessels, where they induce additional local clotting and thereby produce new binding sites for more particles. This amplification system enhanced homing of the nanoparticles in a mouse tumor model without causing clotting or other obvious side effects elsewhere in the body. The self-amplified tumor accumulation produced enhancement of tumor imaging, but significant inhibition of tumor growth was not obtained. We set out to develop an effective theranostic system based on the earlier findings using prostate cancer as the target tumor.

Methods

Cell lines and tumors

The 22Rv1 prostate cancer cell line was obtained from ATCC (Manassas, VA). The cells were grown in RPMI 1640 media supplemented with 2mM glutamine, 1% penicillin-streptomycin, and 10% fetal calf serum at 37°C and 5% CO_2. Xenografts were created by injecting BALB/c nude mice with 2×10^6 cells in phosphate-buffered saline (PBS) orthotopically into the prostate gland. The LAPC9 human prostate adenocarcinoma xenograft was from Dr Lily Wu (University of California, Los Angeles) and was used to produce tumors as described previously.[23] Animal experimentation was performed according to procedures approved by the Animal Research Committee at the University of California, Santa Barbara, and the Sanford-Burnham Medical Research Institute, San Diego, CA.

Peptide synthesis

Peptides were synthesized with an automatic microwave-assisted peptide synthesizer (Liberty; CEM) using standard solid-phase Fmoc/tBu chemistry with 2-(1H-azabenzotriazol-1-yl)-1,1,3,3-tetramethyluronium hexafluorophosphate (AnaSpec) as the coupling reagent. During synthesis, the peptides were labeled with 5(6)-carboxyfluorescein (FAM; Sigma-Aldrich) with a 6-aminohexanoic acid spacer to separate the dye from the sequence. The peptides were cleaved from the resin with 95% trifluoroacetic acid (Sigma-Aldrich) with 2.5% water and triisopropylsilane (Sigma-Aldrich). Subsequent purification by high-performance liquid chromatography (Gilson) yielded peptides with $>90\%$ purity. The preparation of the nonproteinogenic amino acids used for the synthesis of the *N*/*C*α-methylated CREKA analogs will be reported elsewhere. The synthesis of CRKDKC with an extra N-terminal cysteine used for the chemoselective ligation used in the present work also will be described elsewhere.

Computer modeling

The conformational profiles of the CREKA analogs, which were constructed by replacing each residue (one by one) with its *N*-methyl or *C*α-methyl counterpart, were characterized by Molecular Dynamics simulations. Methodology and clustering analyses were as described in Zanuy et al.[24]

Preparation of nanoworms and Ni-liposomes

Nanoworms,[25] nanoworms coated with peptides, and nickel (Ni)–liposomes were prepared as described previously.[22] The aminated nanoworms were PEGylated with maleimide-5KPEG-NHS (JenKem Technology). In the experiments in which Ni-liposomes were used, the nanoworms were functionalized for subsequent peptide coupling with *N*-(α-maleimidoacetoxy)succinimide ester (AMAS; Pierce). Peptides were conjugated to the nanoparticles with the Michael addition reaction between the thiol from a cysteine in the peptide sequence and the maleimide on the functionalized particles.

In vivo peptide homing

Orthotopic prostate cancers were used when they reached 0.5-1 cm in size. Synthetic peptides labeled with FAM (approximately 200 μg) were injected intravenously into tumor-bearing mice and allowed to circulate for 15 minutes to 3 hours. The mice were perfused with PBS through the heart under anesthesia, and tissues were collected and observed under ultraviolet light (Illumatool Bright Light System LT-9900; Lightools Research) and then processed for immunofluorescence or immunohistochemistry.

In vivo nanoworm injections

To analyze nanoworm biodistribution, mice bearing orthotopic 22Rv1 tumors were injected into the tail vein with nanoworms (5 mg of iron per kilogram of body weight). In homing experiments, the mice were euthanized 5-6 hours after the injection by cardiac perfusion with PBS under anesthesia, and organs were dissected and analyzed for particle homing. In tumor-treatment experiments, nude mice bearing 2-week-old 22Rv1 or LAPC9 orthotopic xenografts (typically approximately 200-250 mm^3 in tumor volume) were injected intravenously with nanoworms in 150 μL of PBS or PBS as a control. The nanoworms were injected every other day for 14 days. The total cumulative dose of iron was 35 mg/kg. At the end of the treatment, the mice were perfused with PBS under anesthesia, and the tumors were harvested. Tumor volume was calculated by the following formula: volume $= (d^2 \times D)/2$, where d is the smallest and D the largest tumor diameter.[26]

Peptide stability

The peptides were conjugated with a linker that bridges the nanoworm and a cysteine residue on the peptide, forming a disulfide by reacting with the orthopyridyl-disulfide group. The peptide-coated nanoworms were injected into animals, and blood was collected 15 minutes and 3 hours after the injection. The plasma was separated and nanoworms were collected by ultracentrifugation (100 000*g* for 10 minutes at 4°C). Proteins bound to the nanoworms were removed by incubation with glycine-HCl, pH 2.8 on magnetic LS columns (magnetic-activated cell separation [MACS] columns; Miltenyi Biotec). The peptides were cleaved from the nanoworm by incubation with 10mM dithiothreitol for 30 minutes at room temperature. The iron oxide was separated from the peptide by ultracentrifugation (100 000*g* for 10 minutes at 4°C), and the supernatant fractions containing the peptide were analyzed by matrix-assisted laser desorption ionization–time-of-flight mass spectrometry.

Immunofluorescence and immunohistochemistry

Tissues from mice injected with nanoparticles were fixed in 4% paraformaldehyde overnight at 4°C, cryoprotected in 30% sucrose overnight, and frozen in optimal cutting temperature (OCT) embedding medium. For histologic analysis, 7-μm sections were cut, and sections were stained with hematoxylin and eosin.

For immunostaining, tissue sections were first incubated for 1 hour at room temperature with 10% serum from the species in which the secondary antibody was generated, followed by incubation with the primary antibody overnight at 4°C. The following antibodies were used: rat monoclonal anti–mouse CD31 (10 μg/mL; BD Pharmingen) and mouse fibrin(ogen) antiserum (1:100; Nordic). The primary antibodies were detected with Alexa 647 goat anti–rat and 647 donkey anti–goat secondary antibodies (1:1000; Molecular Probes). Each staining experiment included sections stained only with secondary antibodies as negative controls. Nuclei were counterstained with DAPI (4′,6-diamidino-2-phenylindole; 5 μg/mL; Molecular Probes). The sections were mounted in gel/mount mounting medium (Biomeda) and viewed under a FluoView 500 confocal microscope (Olympus America; 200 micron micrographs, 20× magnification and 50 microns, 40×).

For immunohistochemical staining of frozen tissue sections, endogenous peroxidases were quenched with 3% H_2O_2 (DakoCytomation). Sections were blocked for 1 hour in 5% donkey serum in DakoCytomation antibody dilution solution. Sections were treated with Dako biotin/avidin blocking system and incubated overnight at 4°C with mouse fibrin(ogen) antiserum. The primary antibody was detected with biotinylated anti-mouse immunoglobulin G and a Vectastain ABC kit (Vector Laboratories). Nuclei were counterstained with hematoxylin (Vector Laboratories). To quantify

the homing area of fibrin(ogen) within tumors, the stained sections were scanned with a Scanscope CM-1 scanner and analyzed with ImageScope software41 (Aperio Technologies). Apoptosis was determined with the terminal deoxynucleotidyl transferase–mediated deoxyuridine triphosphate nick-end labeling (TUNEL) assay for the identification of double-stranded DNA breaks with an in situ cell death detection kit (Roche Applied Science) according to the manufacturer's instructions.

Magnetic resonance imaging

Nude mice bearing 22Rv1 orthotopic human prostate cancer xenografts were injected intravenously with superparamagnetic iron oxide nanoworms coated with peptides or nanoworms that were left uncoated at a dose of 5 mg of iron per kilogram of body weight. Each animal received Ni-liposomes (0.2 nmol Ni) intravenously 1 hour before the nanoworms were injected to increase the blood half-life of the nanoworms. Approximately 7-8 hours after the nanoworm injection, the mice were anesthetized with isoflurane and subjected to T2-weighted magnetic resonance imaging scans with a 3-Tesla magnetic resonance imager (GE Healthcare Technologies). After imaging, tissues of interest were harvested and processed for immunofluorescence.

Contrast-enhanced ultrasound

Definity contrast agent (Lantheus Medical Imaging; 5 μL in 45 μL of saline) was injected into the tail vein of mice with a 28-gauge insulin syringe. A Philips iU22 ultrasound system with an L12-5 transducer was used for imaging with a low-mechanical-index, contrast-specific imaging mode (power-modulation mode). The imaging parameters were set as follows and kept identical throughout the study: depth 2 cm, focus zone 2 cm, mechanical index 0.06, 5 frames per second. A 2-minute cine loop was saved for time-intensity curve analysis with Philips QLab. Contrast-enhanced ultrasound (CEUS) was performed before and 1, 3, and 6 hours after injection of mice with nanoworms coated with the CREKA peptide (CREKA-NWs) alone or in combination with nanoworms coated with CRKDKC (CRKDKC-NWs). The tumor rim and center and the surrounding tissue were examined separately to quantify the efficiency of tumor circulation. CEUS analysis of tumors treated for 2 weeks with the nanoworms was performed with Photoshop with a threshold method in which the pixels with enhancement and those without were counted (the threshold was set arbitrarily, because there was no fixed number). The percentage area with enhancement was equal to the pixel number of the enhanced area divided by the pixel number of the entire tumor ×100.

Statistical analysis

Data were analyzed by 2-tailed Student unpaired *t* test or 1-way analysis of variance followed by a suitable post hoc test. *P* values of less than .05 were considered statistically significant.

Results

Nanoworm combinations for enhancement of the activity of CREKA nanoparticles

We used elongated iron oxide nanoparticles, "nanoworms," which are more effective in peptide-mediated cell binding than spherical particles.[25] CREKA-NWs accumulated in the vessels of orthotopic 22Rv1 human prostate cancer xenograft tumors and caused clotting in them, as evidenced by the presence of fibrin(ogen)-containing deposits in the vessel lumens (Figure 1A). In tumors of untreated mice (not shown) or mice treated with nanoparticles coated with peptides other than CREKA, mainly the blood vessel walls were positive for fibrin(ogen) (Figure 1B). Most of the increased fibrin(ogen) staining in the CREKA-NW–treated 22Rv1 tumors was in the tumor periphery, whereas little nanoworm accumulation or clotting was seen in the center of the tumors.

We hypothesized that it might be possible to improve the tumor delivery of nanoworms by combining CREKA with a tumor-homing peptide that recognizes a target molecule other than CREKA and therefore potentially binds to different vessels in the tumor. We tested 2 tumor-homing peptides for their ability to increase CREKA-NW homing: CRKDKC, which was originally identified as a wound-homing peptide,[27] and CGKRK.[28] Both peptides bind to the blood vessels in various types of tumors.[27,28] Both CRKDKC-NWs and CGKRK-NWs accumulated in more than 70% of the 22Rv1 tumor vessels, as evidenced by colocalization with CD31 staining (Figure 1B; supplemental Figure 1, available on the *Blood* Web site; see the Supplemental Materials link at the top of the online article).

We next tested nanoworms double-coated with CREKA and one of the other peptides; however, the double-coated nanoworm showed only minimal tumor homing (supplemental Figure 2). It may be that coating the nanoparticles with 2 different peptides on the same nanoparticle reduces the surface density of each peptide to an extent that adversely affects the homing. Surprisingly, we found that mixtures of CREKA-NWs with CRKDKC-NWs or CGKRK-NWs, which were used as controls, were quite effective in delivering CREKA-NWs to vessels in the tumor interior and causing clotting in them. The mixed single-peptide particles may aggregate in tumor vessels, making it possible for each peptide to carry both types of particles to the target. Among the particle mixtures, the CREKA-CRKDKC mixture was particularly effective in homing to the entire tumor (Figure 1C), and we subsequently focused on this combination. Quantification of fibrin(ogen) accumulation showed that the combination of CREKA-NWs with CRKDKC-NWs enhanced clotting by 4- to 5-fold compared with CREKA-NWs alone (Figure 1D). CEUS imaging showed a 90% reduction in blood flow at 6 hours after injection of the nanoworm mixture (Figure 2).

Enhancing the activity of CREKA by incorporation of noncoded amino acids

We hypothesized that protecting CREKA against proteolytic degradation may further increase the efficacy of the tumor homing. Proteolysis protection can be achieved through the incorporation of nonproteinogenic amino acids, provided that the bioactive conformation of the peptide is retained.[24,29] On the basis of molecular modeling studies,[24] several *N*- and *C*α-methylated amino acids were selected to replace the key residues in CREKA. This chemical modification can be viewed as the methylation in certain positions of the peptide backbone (at either N or Cα). These studies indicated that the *N*- and *C*α-methylation of the Arg, Glu, and Lys residues does not affect the conformational profile of the peptide (supplemental Figure 3). The CREKA analogs that incorporated the *N/C*α-methylated amino acids were synthesized as fluorescein (FAM)–labeled peptides. Several of the CREKA analogs showed significantly higher accumulation in the tumors than unmodified CREKA (Figure 3A). An exception was C(*N*Me)REKA, in which the arginine residue is *N*-methylated; this peptide gave only weak tumor fluorescence. Confocal microscopy confirmed the organ-level analyses [shown for CR(*N*Me)EKA in 22Rv1 tumors in Figure 3B and for LAPC9 tumors in Figure 3C]. The active CREKA analogs displayed a meshwork pattern within both the viable and the necrotic lesions of tumor stroma that was stronger and more extensive than that seen with CREKA. As expected, staining of tumor sections with antibodies against fibrin(ogen) and fibronectin showed that the CREKA analogs accumulated in areas

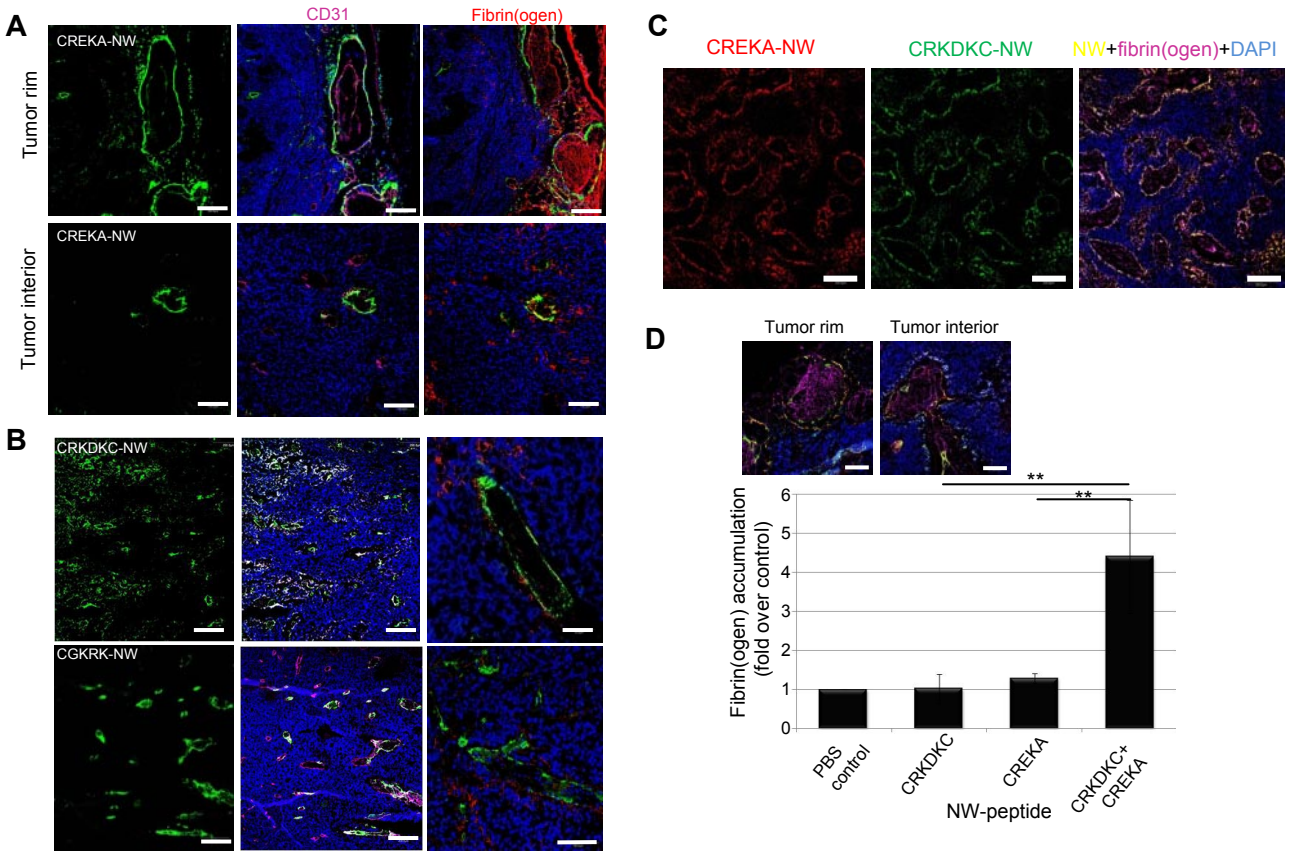

Figure 1. Combining CREKA-NWs with nanoworms coated with another tumor-homing peptide enhances homing efficiency. (A) Iron oxide nanoworms coated with FAM-labeled CREKA peptide were injected intravenously (5 mg of iron per kilogram of body weight) into nude mice bearing orthotropic 22Rv1 human prostate tumors. The mice had been preinjected with Ni-liposomes to reduce uptake by the reticuloendothelial system.[22] Tumors were harvested 5 hours later, and tumor sections were stained with antibodies and examined by confocal microscopy (the 5-hour time point was found to be optimal for nanoworm homing with regard to accumulation of the nanoworms in the tumor and clearance of nanoworms from the blood). The CREKA-coated particles are green; blood vessels and clotting were visualized separately with anti-CD31 (magenta) or antifibrin(ogen) staining (red); nuclei were stained with DAPI (blue). Bars represent 200 μm. (B) Nanoworms coated with FAM-labeled CRKDKC or CGKRK were injected intravenously, and the tissues were collected and processed as in panel A. CRKDKC- or CGKRK-coated particles are green; blood vessels visualized with anti-CD31 are magenta (white indicates colocalization of magenta and green) and those visualized with anti-fibrin(ogen) staining are red (yellow indicates colocalization of red and green); nuclei were stained with DAPI (blue). Large vessels were selected for the panels on the right because intravascular clotting (which is not promoted by CRKDKC-NWs or CGKRK-NWs) is most apparent in larger vessels. Bars represent 200 μm (left and middle panels) and 100 μm (right panels). (C) A mixture of nanoworms coated with rhodamine-labeled CREKA (red) and FAM-labeled CRKDKC (green) was injected intravenously (2.5 mg of iron per kilogram of each nanoworm preparation), and the tissues were collected and processed as in A and stained for fibrin(ogen) (magenta); nuclei were stained with DAPI (blue). Bars represent 200 μm. (D) Mice were injected with the indicated materials as in panels A, B, or C. The sections stained with anti-fibrin(ogen) antibody were subjected to image analysis with Scanscope to quantify fibrin(ogen)-positive areas. The insets show examples of anti-fibrin(ogen) immunostaining in the tumor rim (left) and interior (right) from mice injected with the nanoworm mixture. Bars represent 50 μm. Statistical analyses were performed with analysis of variance. Error bars represent SEM (n = 5-6); $^{**}P < .01$.

rich in deposition of these proteins (Figure 3B, right panels). CR(*N*Me)EKA and CRE(*C*αMe)KA appeared to be equally active in this regard (Figure 4).

To investigate the stability of CREKA and CR(*N*Me)EKA in the tumor in vivo, these peptides were injected intravenously into mice bearing 22Rv1 tumors. The peptides yielded equally strong fluorescence in the tumors 30 minutes after the injection (Figure 3D); however, after 3 hours, the CREKA fluorescence had decreased by 70%, whereas CR(*N*Me)EKA showed no significant decrease and greater stability. On the basis of these observations, we selected the backbone-methylated peptides CR(*N*Me)EKA and CRE(*C*αMe)KA for studies with nanoparticles.

Intratumoral distribution of iron oxide nanoworms coated with CREKA analogs

Intravenously injected CRE(*C*αMe)KA-NWs and CR(*N*Me)EKA-NWs showed greatly enhanced accumulation in the blood vessels of the tumor rim and interior (Figures 4-5A). These areas were also positive for antifibrin(ogen) staining. This distribution of the nanoworms coated with the *N/C*α-methylated peptides within tumors was markedly different from CREKA-NWs, in which the nanoparticles appeared less abundant in the interior of tumors (compare Figures 4 and 5A with Figure 1A). No fluorescence from the various nanoworm formulations was observed in normal tissues of the tumor-bearing mice, with the exception of the liver and the spleen, which nonselectively take up all nanoparticles. The liver accumulation of these nanoworms was similar (shown for CR(*N*-Me)EKA-NWs in supplemental Figure 4). Significantly more tumor accumulation of CR(*N*Me)EKA-NWs than CREKA-NWs was also observed in a different prostate cancer xenograft model, LAPC9 (supplemental Figure 5).

Magnetic resonance imaging of 22Rv1 tumor mice after intravenous injection of nanoworms showed hypointense vascular signals throughout the tumor for the CR(*N*Me)EKA-NWs and similar but weaker signals with CREKA-NWs (Figure 5B). Nontargeted nanoworms gave no detectable signal in these tumors after most of the nanoparticles had been cleared from the blood.[30]

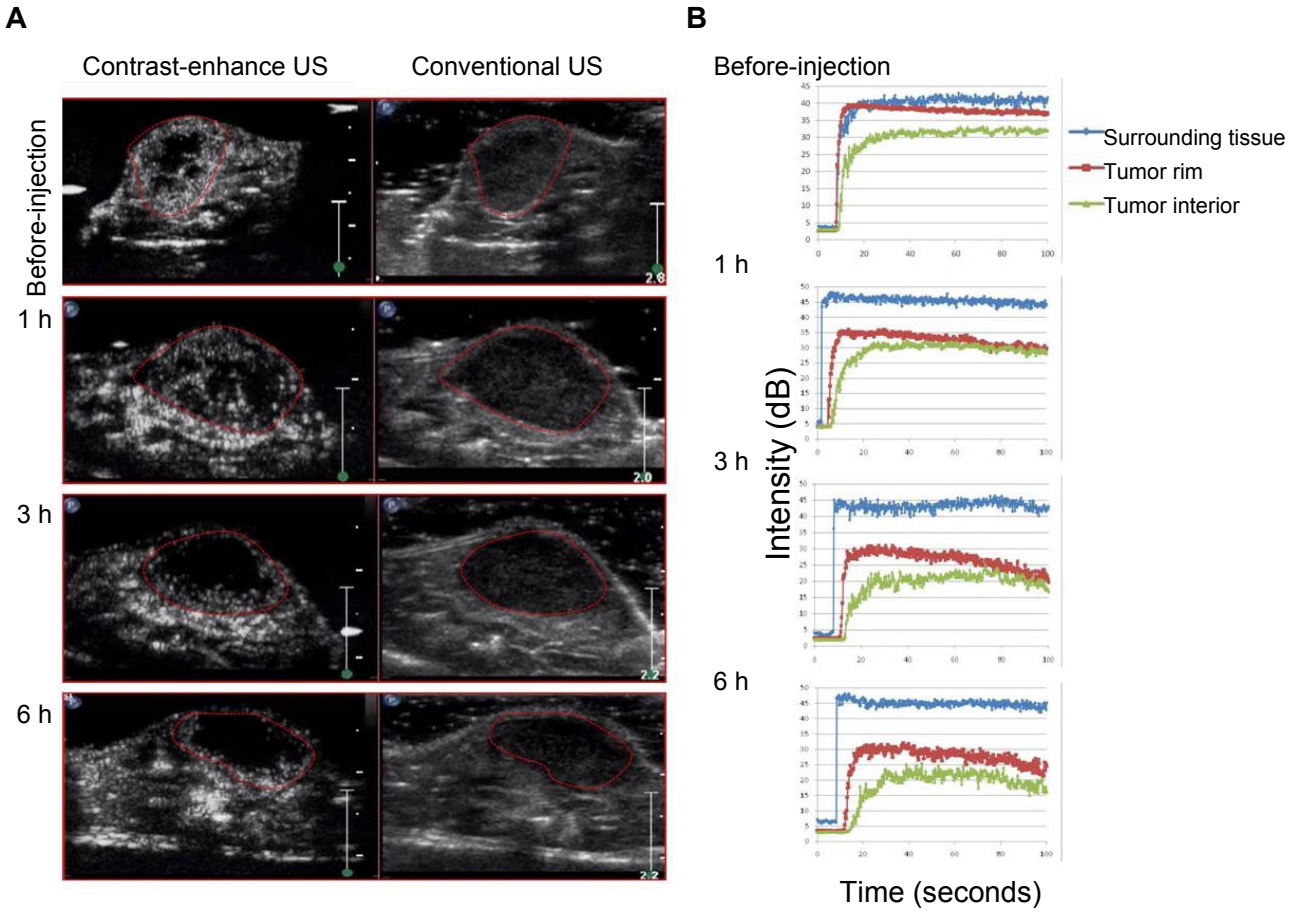

Figure 2. CEUS imaging of blood circulation in tumors of mice treated with peptide-coated nanoworms. (A) Mice preinjected with Ni-liposomes were subsequently injected with a mixture of CREKA-NWs and CRKDKC-NWs and, after the indicated periods of time, injected with an ultrasound contrast agent. CEUS and conventional ultrasound (US) images obtained at the different time points are shown. The images are representative of 3 tumors imaged. (B) Enhancement-analysis curves of blood flow in different tumor regions and the surrounding tissue from experiments described in panel A. The orientation of the tumors is slightly different between the time points because the mice were anesthetized for each scan and reintroduced to the ultrasound instrument; n = 3.

Therapeutic efficacy of tumor blood vessel blockage by peptide-coated nanoworms

Having optimized the CREKA self-amplified targeting system by combining CREKA-NWs with CRKDKC-NWs and by incorporation of *N*/*C*α-methylated amino acids, we tested the tumor-treatment potential of the enhanced system. The Ni-liposome pretreatment we used in the short-term experiments to block liver uptake of nanoworms was not suitable for the long-term treatment experiments; it would have doubled the number of injections needed, and we also observed some deaths among mice that received multiple injections of Ni-liposomes. We omitted the liposome pretreatment and instead coated the nanoworms with polyethylene glycol (PEG) and coupled the homing peptide to the nanoparticles through the PEG chains.

We used the peptides bound to the nanoworms through PEG to directly compare the in vivo stability of CREKA and CR(*N*Me)EKA. The peptides were coupled through a reversible disulfide linkage to the PEG coating, and the coated nanoworms were injected intravenously into mice bearing 22Rv1 tumors. The nanoworms were recovered from the blood, and the peptides were isolated and analyzed by mass spectrometry. CREKA and CR(*N*Me)EKA were equally abundant in the blood samples obtained after 15 minutes of circulation (supplemental Figure 6); however, after 3 hours, CREKA was undetectable, which indicates that all of the peptide was degraded, whereas the amount of CR(*N*Me)EKA only declined by approximately 60%. These results show that, as intended by the chemical modification, CR(*N*Me)EKA is more stable in vivo than CREKA. CR(*N*Me)EKA bound to plasma clots with somewhat higher affinity than CREKA (K_d = 2.5μM and 6.0μM, respectively; supplemental Figure 7), which suggests that affinity may also contribute to the superior homing properties of the methylated peptide.

There was some loss of homing activity and clotting in tumor vessels compared with the PEG-free nanoparticles. We hypothesized that multiple injections might compensate for this reduced activity. Indeed, many of the blood vessels around the necrotic area in the tumors of the mice treated for 2 weeks with the nanoworm combination were filled with peptide particles and deposits positive for fibrin(ogen) immunostaining (Figure 6A; supplemental Figure 8). Moreover, CEUS analysis of tumors treated with the nanoworms revealed a reduction in tumor blood flow; CR(*N*Me)EKA-PEG-NWs alone gave a 30% reduction, and the combination of CR(*N*Me)EKA-PEG-NWs with CRKDKC-PEG-NWs more than doubled the effect (Figure 6B; supplemental Figure 9).

Histologic analysis of tumors from mice treated with CR(*N*Me)EKA-PEG-NWs in combination with CRKDKC-PEG-NWs showed extensive necrosis, as evidenced by a typical loss of nuclei in the center of the tumors (Figure 6C). No signs of apoptosis or necrosis were observed in similarly sized tumors in the control groups (CRKDKC-PEG-NW and PBS). TUNEL staining

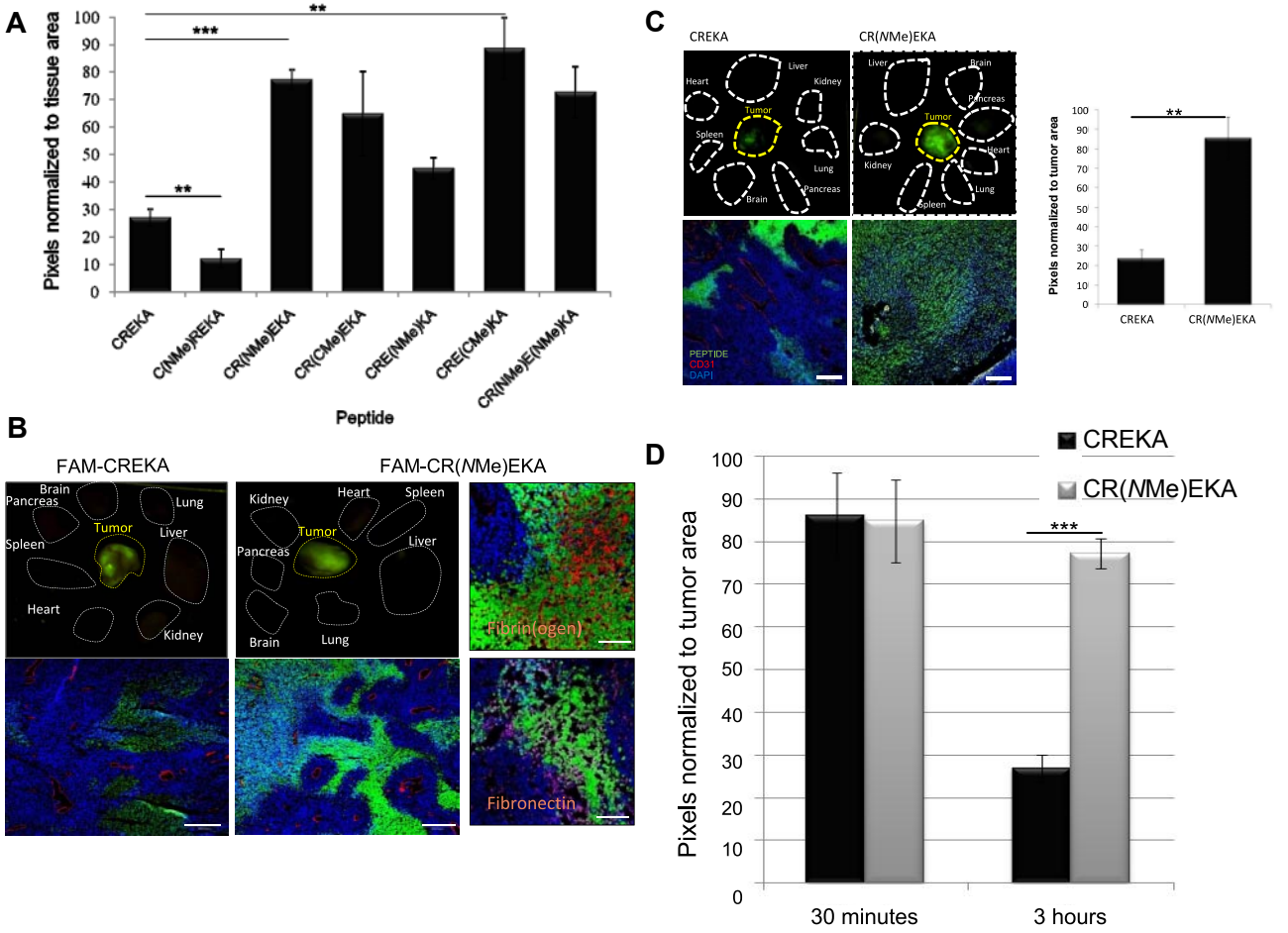

Figure 3. Tumor accumulation of the CREKA peptide and its *N*/*C*α-methylated variants. Mice bearing orthotropic 22Rv1 xenograft tumors were injected intravenously with 200 μg of FAM-labeled CREKA or *N*/*C*α-methylated CREKA peptides, which were allowed to circulate for 3 hours. This time point highlights the differences between nonmodified CREKA and some of the methylated variants (D). The mice were perfused through the heart with PBS, and the organs shown were collected and viewed under ultraviolet light. (A) Quantification of fluorescence with ImageJ software. Several *N*/Cα-methylated CREKA analogs produced stronger fluorescence than unmodified CREKA. Statistical analyses were performed with analysis of variance. Error bars show SEM (n = 3-4); $^{**}P < .01$; $^{***}P < .001$. (B-C) Representative images from mice injected with the CREKA or CR(*N*Me)EKA peptides (B, 22Rv1 xenografts; C, LAPC9 xenografts). In the top panels, white dotted lines show where the organs were placed in a macroscopic examination, and the yellow lines outline the tumor. The bottom panels show confocal images of tumor sections from mice injected with the peptides (green) indicated above. Blood vessels were visualized with anti-CD31 (red); nuclei were stained with DAPI (blue). Bars represent 200 μm. (B right panels) Representative confocal image fields illustrate the localization of the CR(*N*Me)EKA peptide (green) in relation to anti-fibrin(ogen) (red) and anti-fibronectin (magenta) staining used as markers of tumor stroma; nuclei were stained with DAPI (blue). Bar represents 50 μm. (C right panels) Quantification of fluorescence with ImageJ software. Statistical analysis was performed with Student *t* test. Error bars show SEM (n = 3); $^{**}P < .01$. (D) Quantification of fluorescence with ImageJ software 15 minutes or 3 hours after peptide injection into 22Rv1 tumor–bearing mice. CR(*N*Me)EKA produced stronger fluorescence over time than unmodified CREKA. Statistical analysis was performed with Student *t* test. Error bars show SEM (n = 3-4); $^{***}P < .001$. (*N*Me) and (*C*Me) indicate an *N*- or *C*α-methylated residue, respectively.

revealed extensive apoptosis in the surviving areas of the tumors treated with the CR(*N*Me)EKA-PEG-NW and CRKDKC-PEG-NW combination (Figure 6D). There was highly significant inhibition of tumor growth in the mice treated with the combination compared with mice that received PBS or CRKDKC-PEG-NW alone (Figure 7A). CR(*N*Me)EKA-PEG-NW alone showed a modest but significant inhibition of tumor growth. The CR(*N*Me)EKA-PEG-NW and CRKDKC-PEG-NW combination treatment also inhibited tumor growth in LAPC9 tumor mice, producing a significant survival increase compared with mice treated with vehicle alone (Figure

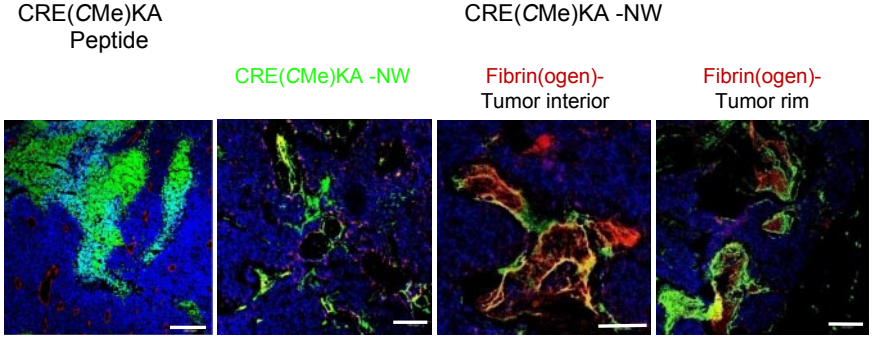

Figure 4. CRE(CMe)KA-NW homing to 22Rv1 tumors. Mice bearing orthotropic 22Rv1 xenograft tumors were injected intravenously with 200 μg of FAM-labeled CRE(*C*Me)KA or 5 mg of iron per kilogram of nanoworms coated with FAM-CRE(*C*Me)KA. The peptide was allowed to circulate for 3 hours, and nanoworms were allowed to circulate for 5 hours. The mice were then perfused through the heart with PBS, and the tumors were collected. Tumor sections were stained with CD31 or anti-fibrin(ogen) (red) and examined by confocal microscopy. Nanoworms are green; nuclei were stained with DAPI (blue). Bars represent 200 μm. n = 3.

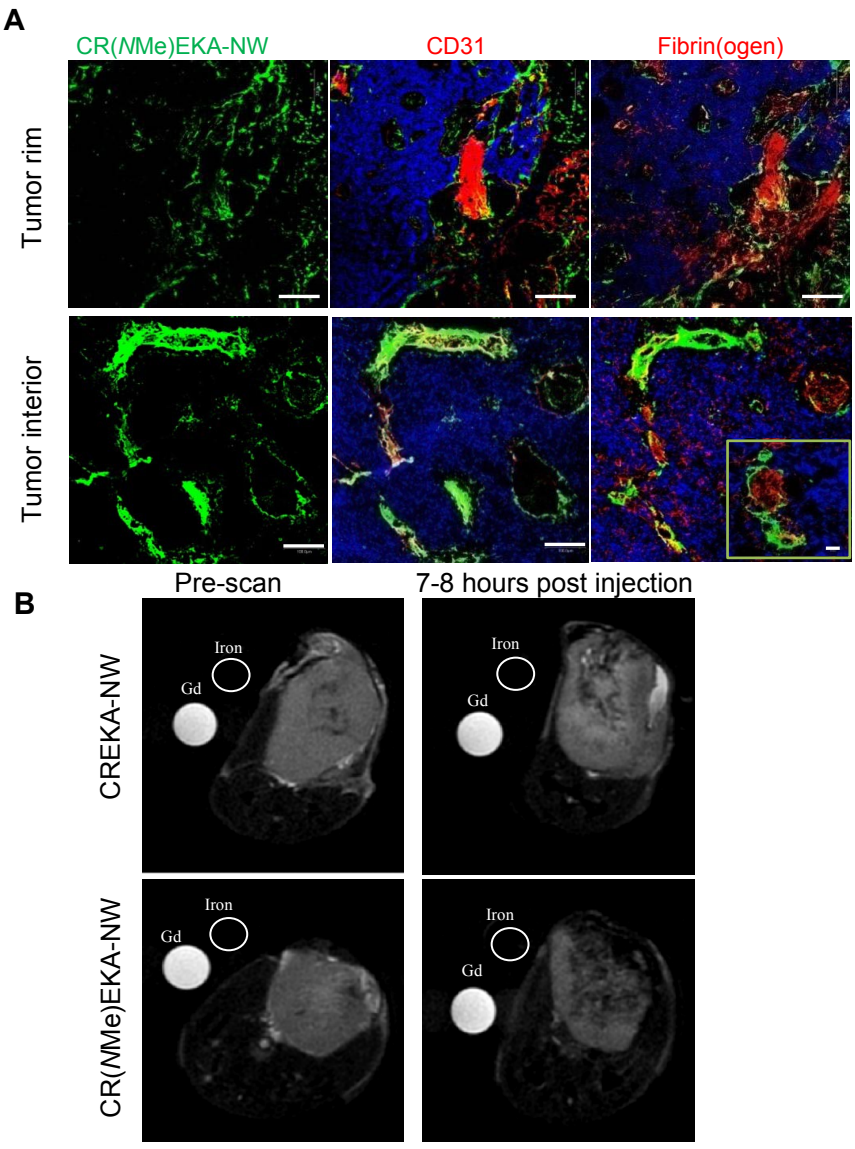

Figure 5. Improved tumor homing of nanoworms coated with an *N*-methylated CREKA peptide analog. Nanoworms coated with FAM-labeled CREKA peptide or its *N*-methylated variant, CR(*N*Me)EKA, were injected intravenously into mice bearing 22Rv1 tumors (total dose 5 mg of iron per 1 kg). (A) Tumors were harvested 5 hours later, and tumor sections were stained with antibodies and examined by confocal microscopy. CR(*N*Me)EKA-NWs are green; blood vessels and clotting were visualized separately with anti-CD31 or anti-fibrin(ogen) staining (red). Nuclei were stained with DAPI (blue). Bars represent 100 μm (50 μm in the inset). (B) T2-weighted magnetic resonance images (fast spin echo, repetition time = 6.4 seconds, echo time = 69 ms). CREKA-NWs or CR(*N*Me)EKA-NWs were injected intravenously into tumor-bearing mice. The particles were allowed to circulate for 7-8 hours (the time determined in preliminary experiments to be optimal for differential homing). Gray-scale images of axial planes through the tumors are shown. Gadolinium (Gd) and Feridex (iron) were used as reference standards. n = 3-4.

7B). These treatments showed no obvious systemic toxicity, as evidenced by body weight measurements and histologic analysis of organs from the treated mice. No signs of blood clotting elsewhere in the body (eg, sudden death or paralysis due to stroke, pulmonary embolism, or deep vein thrombosis) or signs of disseminated intravascular coagulation were observed.

Discussion

Our results establish a tumor treatment and imaging strategy that is based on synergistic and self-amplifying accumulation of homing peptide–coated iron oxide nanoworms in prostate tumor blood vessels. We show that extensive coverage of tumor vessels can be achieved by combining nanoparticles that are coated with either of 2 tumor-homing peptides, CREKA or CRKDKC. We also show that protecting the CREKA peptide against proteolysis through the incorporation of *N*/*C*α-methylated residues increases the ability of the CREKA-NWs to home to tumor blood vessels and to cause clotting in them. The combination of the 2 approaches allowed effective magnetic resonance imaging of the tumors and produced extensive inhibition of tumor growth.

The changes we introduced into the CREKA self-amplifying tumor-vessel–homing system[22] revealed surprising cooperation of 2 nanoparticle species coated with different peptides. We had assumed that to achieve greater coverage of prostate cancer vessels, the 2 peptides should be on the same particle, but we found that having them on separate particles was more effective. Coaccumulation with CREKA-NWs was not limited to the CRKDKC peptide; nanoworms coated with another tumor-homing peptide, CGKRK, also enhanced the accumulation of CREKA-NWs in tumor vessels, albeit not as strongly as CRKDKC-NWs. A likely explanation for this phenomenon is coaggregation of the 2 species of nanoparticles, which apparently only happens at the high concentrations of nanoworms achieved within tumor vessels. The clotting induced by the CREKA-NWs may contribute to the coaccumulation by trapping loosely bound CRKDKC-NWs that would otherwise be washed away by the blood flow. Another cooperative 2-particle nanosystem has been described recently.[31]

The prothrombotic activity of the CREKA-NW is selective for tumors. This is attributable in part to the selective accumulation of CREKA-NWs, and the nanoworm mixture, in tumor vessels. Both the peptide and the iron oxide component of the nanoparticles are responsible for the thrombotic activity, because other types of

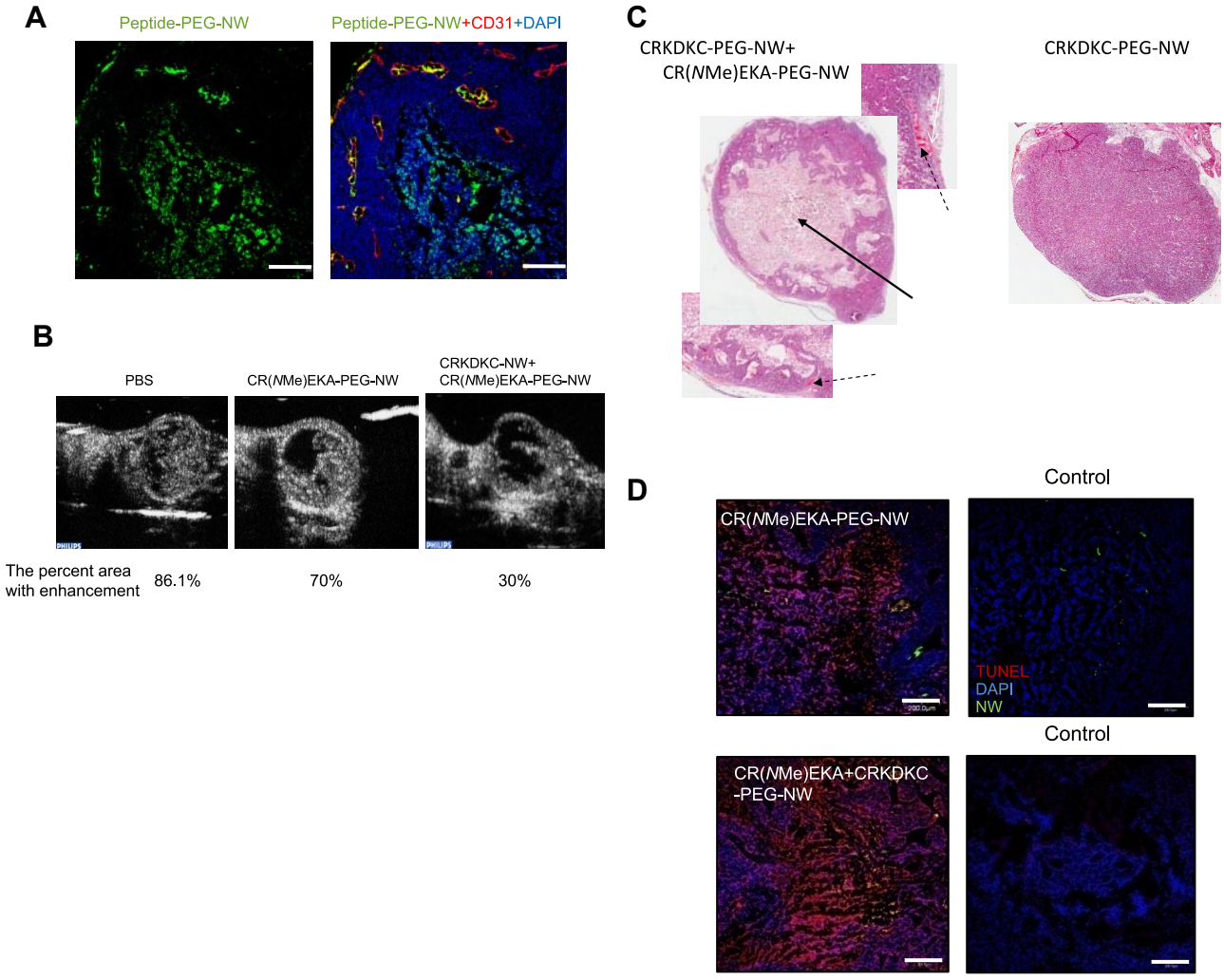

Figure 6. Nanoworm distribution and effects on intravascular clotting, tumor apoptosis, and tumor therapy. Mice bearing 2-week-old orthotopic xenografts of 22Rv1 human prostate cancer were injected intravenously with nanoworms coated with peptides through a 5-kDa PEG spacer. The nanoworms were administered every other day for 14 days (5 mg of iron per kilogram per day, total cumulative dose 35 mg/kg). (A) Tumor sections were stained with anti-CD31 (red); CR(*N*Me)EKA-NW/CRKDKC-NW combination is shown as green; nuclei were stained with DAPI (blue). Bars represent 200 μm. The necrotic area at the center of the tumor is autofluorescent. (B) CEUS imaging and analysis showed reduction in tumor blood flow at the end of treatment. The images are representative of n = 3. (C) Staining with hematoxylin and eosin showed a large necrotic area (arrow) in the middle of a typical tumor treated with the CR(*N*Me)EKA-NW/CRKDKC-NW combination and occluded vessels in the viable rim of these tumors (broken arrows). A tumor of a similar size from a mouse treated with CRKDKC-NWs alone is shown for comparison. (D) Apoptosis analysis by TUNEL staining is shown as red; nanoworm combination is shown as green; nuclei were stained with DAPI. Bars represent 200 μm.

nanoparticles coated with CREKA and the free CREKA peptide lack this activity,[26,32] and iron oxide nanoworms coated with tumor-homing peptides other than CREKA (CRKDKC and CGKRK) also do not cause clotting. Iron oxide nanoparticles are known to be procoagulants, and the affinity of CREKA for clotting products apparently enhances that activity. The nanoworm, like other nanoparticles, nonspecifically accumulates in the liver and spleen.[33] However, we did not observe any clotting in the normal tissues of the tumor mice in the present study or in an earlier study that used a similar but less effective system.[22] Thus, the tumor environment, which is procoagulant,[19,20] is also likely to play a role in bringing about clotting in tumor vessels. Atherosclerotic plaques tend to show subtle spontaneous clotting.[32,34] Thus, the presence of atherosclerosis could be a limitation in the clinical application of the CREKA technology.

The potential of peptides as drug candidates is limited by poor pharmacokinetics, which includes rapid elimination from the circulation through filtration into the urine and susceptibility to proteolysis. Elimination into the urine is not a problem with peptides coated onto a nanoparticle, but the present results do demonstrate the importance of proteolysis. Because each nanoparticle is coated with multiple peptides, one might expect the nanoparticle coating to tolerate some proteolysis without significant loss of activity. The present results indicate that this is not the case; protecting the peptide against proteolytic cleavage by incorporating noncoded amino acids substantially improved the tumor-homing efficiency and increased the blockade of tumor vessels. Direct measurement of the stability of the peptides in vivo supported the conclusion that increased peptide stability is responsible, at least in part, for the improved characteristics of the methylated CREKA analogs. If extended to other peptide-coated nanoparticles, this result could have significant implications for the design of effective nanoparticle therapies.

In the present study, we show antitumor activity of our system against 2 orthotropic prostate cancer xenograft tumors, 22Rv1 and LAPC9. It is likely that other tumor types can be similarly targeted, because we have shown other types of tumors to be targeted by the CREKA system.[22] The efficiency of the combined CREKA-NWs

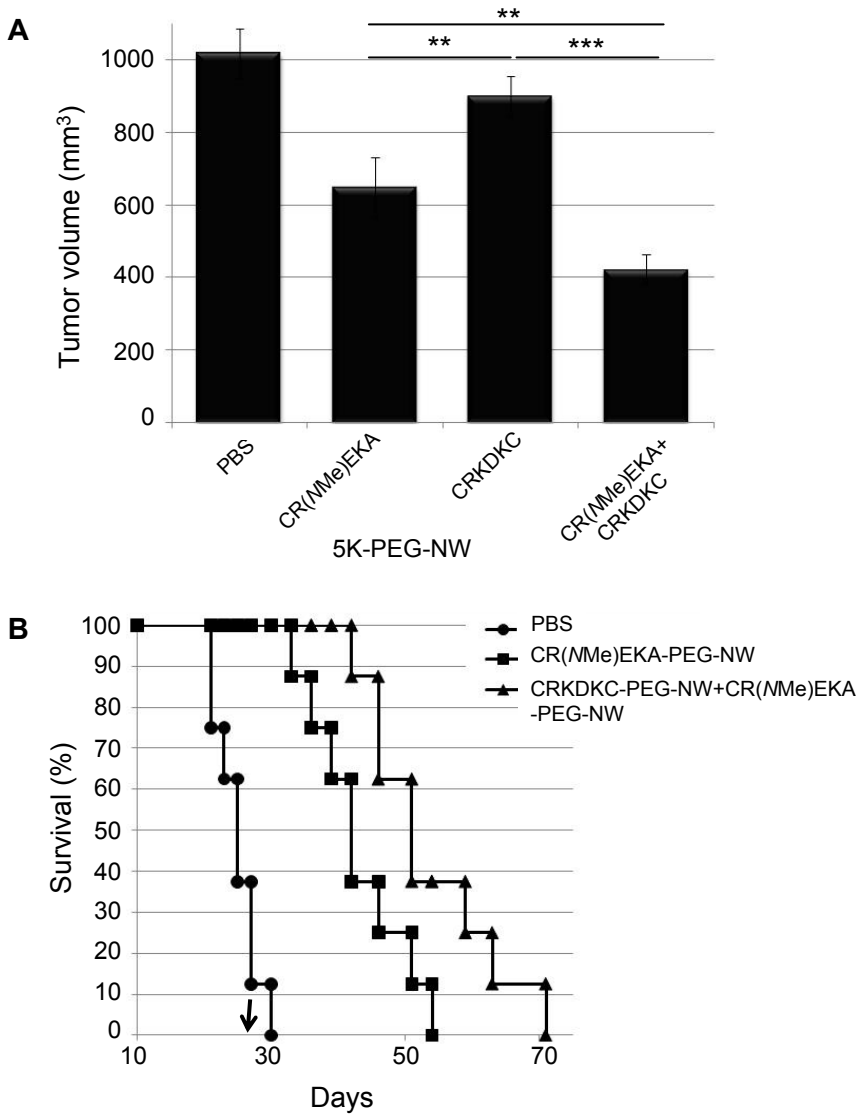

Figure 7. Tumor treatment with targeted nanoworms. Mice bearing orthotopic xenografts of 22Rv1 or LAPC9 human prostate cancer (2 weeks or 10 days after inoculation, respectively) were injected intravenously with nanoworms coated with peptides through a 5-kDa PEG spacer. The particles were administered every other day for 14 days (5 mg of iron per kilogram per day, total cumulative dose 35 mg/kg). (A) Tumor volume 1 day after the last injection in the 22Rv1 model is shown. Statistical analyses were performed with analysis of variance. Error bars show SEM (n = 10-12); $^{**}P < .01$; $^{***}P < .001$. Similar results were obtained in 2 independent experiments. (B) Mice bearing LAPC9 tumors were treated as described in panel A, and survival was monitored over time (n = 8 per group). The arrow indicates the day the nanoworm treatment was stopped.

strongly correlated with the degree of tumor vessel blockade achieved with the various treatments. CR(*N*Me)EKA-PEG-NWs caused 30% reduction in tumor blood flow, as documented by CEUS, and produced a modest reduction in tumor size. The CRKDKC-PEG-NW and CR(*N*Me)EKA-PEG-NW combination blocked 70% of tumor blood flow and produced a strong reduction in tumor size, as well as extended survival of the animals. Significantly, these results were obtained using only the inherent properties of the nanoworm, which also allowed imaging of the tumors. The addition of a drug to the particles could further enhance the utility of this theranostic nanosystem.

Acknowledgments

We thank Dr Jerry Lee for discussions. Jacqueline Corbeil helped with magnetic resonance imaging, Dr Gema Ballano with the syntheses, and Guillem Revilla-Lopez with simulations. The Center de Supercomputacio de Catalunya and the Barcelona Supercomputing Center provided computational facilities.

This work was supported by National Cancer Institute grants (P01-CA104898 [E.R.], P01-CA124427 [M.J.S., E.R.], and P01-CA119335 [R.F.M., M.J.S., E.R.]); Cancer Center support grant CA 30199, P50-CA128346 to the University of California at San Diego In Vivo Cancer Molecular Imaging Center; and grants CTQ2008-00423-E/BQU and CTQ2007-62245 (A.I.J., C.C., C.A.) from the Spanish Ministerio de Ciencia e Innovacion. This project has been funded in part with federal funds from the National Cancer Institute, National Institutes of Health, under contract no. HHSN261200800001E. This research was supported in part by the Intramural Research Program of the National Institutes of Health, National Cancer Institute, Center for Cancer Research.

The content of this publication does not necessarily reflect the views or policies of the Department of Health and Human Services, nor does mention of trade names, commercial products, or organizations imply endorsement by the US government.

Authorship

Contribution: L.A., K.N.S., A.I.J, C.C., C.A., R.N., and E.R. designed the experiments; L.A. and K.N.S. conducted the biochemical and animal experiments; L.A., V.R.K., and K.G. synthesized nanoworms; V.R.K. participated in the design of the synthetic

peptides, performed the syntheses, and analyzed the mass spectrometry data; K.N.S, O.M.G., Y.K., and R.F.M provided the imaging technologies; J.-H.P and M.J.S. designed the iron oxide nanoworms; A.I.J., C.C., D.Z., F.J.S., C.A., and R.N. performed computer simulation analyses on the structure of CREKA, helped design the *N/C* methylated peptides, and provided the *N/C* methylated amino acid precursors for peptide synthesis; A.I.J., C.C., D.Z., F.J.S., C.A., and R.N. performed computer simulation analyses on the structure of CREKA, designed the peptide analogs, and provided the *N/C*α-methylated amino acids; and L.A. and E.R. wrote the manuscript. All authors discussed the results and commented on the manuscript.

Conflict-of-interest disclosure: The authors declare no competing financial interests.

Correspondence: Erkki Ruoslahti, Vascular Mapping Laboratory, Center for Nanomedicine, Sanford-Burnham Medical Research Institute at the University of California at Santa Barbara, Santa Barbara, CA 92037; e-mail ruoslahti@burnham.org.

References

1. Jemal A, Siegel R, Ward E, et al. Cancer statistics, 2008. *CA Cancer J Clin.* 2008;58(2):71-96.
2. Macintosh CA, Stower M, Reid N, Maitland NJ. Precise microdissection of human prostate cancers reveals genotypic heterogeneity. *Cancer Res.* 1998;58(1):23-28.
3. Ruijter ET, van de Kaa CA, Schalken JA, Debruyne FM, Ruiter DJ. Histological grade heterogeneity in multifocal prostate cancer: biological and clinical implications. *J Pathol.* 1996; 180(3):295-299.
4. Miller GJ, Cygan JM. Morphology of prostate cancer: the effects of multifocality on histological grade, tumor volume and capsule penetration. *J Urol.* 1994;152(5, pt 2):1709-1713.
5. Jain RK, Munn LL, Fukumura D. Dissecting tumour pathophysiology using intravital microscopy. *Nat Rev Cancer.* 2002;2(4):266-276.
6. Weissleder R. Scaling down imaging: molecular mapping of cancer in mice. *Nat Rev Cancer.* 2002;2(1):11-18.
7. Ruoslahti E, Bhatia SN, Sailor MJ. Targeting of drugs and nanoparticles to tumors. *J Cell Biol.* 2010;188:6759-6768.
8. Folkman J. Angiogenesis in cancer, vascular, rheumatoid and other disease. *Nat Med.* 1995; 1(1):27-31.
9. Ferrara N, Alitalo K. Clinical applications of angiogenic growth factors and their inhibitors. *Nat Med.* 1999;5(12):1359-1364.
10. Folkman J. Angiogenesis: an organizing principle for drug discovery? *Nat Rev Drug Discov.* 2007; 6(4):273-286.
11. Carmeliet P. Mechanisms of angiogenesis and arteriogenesis. *Nat Med.* 2000;6(4):389-395.
12. Beecken WD, Fernandez A, Joussen AM, et al. Effect of antiangiogenic therapy on slowly growing, poorly vascularized tumors in mice. *J Natl Cancer Inst.* 2001;93(5):382-387.
13. Bieker R, Kessler T, Schwoppe C, et al. Infarction of tumor vessels by NGR-peptide-directed targeting of tissue factor: experimental results and first-in-man experience. *Blood.* 2009;113(20):5019-5027.
14. Huang X, Molema G, King S, Watkins L, Edgington TS, Thorpe PE. Tumor infarction in mice by antibody-directed targeting of tissue factor to tumor vasculature. *Science.* 1997; 275(5299):547-550.
15. Kessler T, Bieker R, Padro T, et al. Inhibition of tumor growth by RGD peptide-directed delivery of truncated tissue factor to the tumor vasculature. *Clin Cancer Res.* 2005;11(17):6317-6324.
16. Nilsson F, Kosmehl H, Zardi L, Neri D. Targeted delivery of tissue factor to the ED-B domain of fibronectin, a marker of angiogenesis, mediates the infarction of solid tumors in mice. *Cancer Res.* 2001;61(2):711-716.
17. Ran S, Gao B, Duffy S, Watkins L, Rote N, Thorpe PE. Infarction of solid Hodgkin's tumors in mice by antibody-directed targeting of tissue factor to tumor vasculature. *Cancer Res.* 1998; 58(20):4646-4653.
18. Hoffman JA, Laakkonen P, Porkka K, Bernasconi M, Ruoslahti E. In vivo and ex vivo selections using phage-displayed libraries. In: Clackson T, Lowman HB, eds. *Phage Display: A Practical Approach.* New York, NY: Oxford University Press; 2004:171-191.
19. Abe K, Shoji M, Chen J, et al. Regulation of vascular endothelial growth factor production and angiogenesis by the cytoplasmic tail of tissue factor. *Proc Natl Acad Sci U S A.* 1999;96(15):8663-8668.
20. Dvorak HF, Senger DR, Dvorak AM, Harvey VS, McDonagh J. Regulation of extravascular coagulation by microvascular permeability. *Science.* 1985;227(4690):1059-1061.
21. Pilch J, Brown DM, Komatsu M, et al. Peptides selected for binding to clotted plasma accumulate in tumor stroma and wounds. *Proc Natl Acad Sci U S A.* 2006;103(8):2800-2804.
22. Simberg D, Duza T, Park JH, et al. Biomimetic amplification of nanoparticle homing to tumors. *Proc Natl Acad Sci U S A.* 2007;104(3):932-936.
23. Agemy L, Harmelin A, Waks T, et al. Irradiation enhances the metastatic potential of prostatic small cell carcinoma xenografts. *Prostate.* 2008; 68(5):530-539.
24. Zanuy D, Flores-Ortega A, Jimenez AI, et al. In silico molecular engineering for a targeted replacement in a tumor-homing peptide. *J Phys Chem B.* 2009;113(22):7879-7889.
25. Park JH, von Maltzahn G, Zhang L, et al. Systematic surface engineering of magnetic nanoworms for in vivo tumor targeting. *Small.* 2009;5(6):694-700.
26. Jarvinen TA, Ruoslahti E. Molecular changes in the vasculature of injured tissues. *Am J Pathol.* 2007;171(2):702-711.
27. Hoffman JA, Giraudo E, Singh M, et al. Progressive vascular changes in a transgenic mouse model of squamous cell carcinoma. *Cancer Cell.* 2003;4(5):383-391.
28. Chatterjee J, Gilon C, Hoffman A, Kessler H. N-methylation of peptides: a new perspective in medicinal chemistry. *Acc Chem Res.* 2008; 41(10):1331-1342.
29. Sugahara KN, Teesalu T, Karmali PP, et al. Tissue-penetrating delivery of compounds and nanoparticles into tumors. *Cancer Cell.* 2009; 16(6):510-520.
30. Park JH, von Maltzahn G, Xu MJ, et al. Cooperative nanomaterial system to sensitize, target, and treat tumors. *Proc Natl Acad Sci U S A.* Dec 28 2009.
31. Karmali PP, Kotamraju VR, Kastantin M, et al. Targeting of albumin-embedded paclitaxel nanoparticles to tumors. *Nanomedicine.* 2009;5(1):73-82.
32. Peters D, Kastantin M, Kotamraju VR, et al. Targeting atherosclerosis by using modular, multifunctional micelles. *Proc Natl Acad Sci U S A.* 2009;106(24):9815-9819.
33. Thorek DL, Chen AK, Czupryna J, Tsourkas A. Superparamagnetic iron oxide nanoparticle probes for molecular imaging. *Ann Biomed Eng.* 2006;34(1):23-38.
34. Smith EB. Fibrinogen and atherosclerosis. *Wien Klin Wochenschr.* 1993;105(15):417-424.